Electronic Supplementary Information (ESI)

Advanced hermetic encapsulation of perovskite solar cells: the route to commercialization

Seyedali Emami, Jorge Martins, Dzmitry Ivanou and Adélio Mendes*

LEPABE - Laboratory for Process Engineering, Environment, Biotechnology and Energy, Faculdade de Engenharia, Universidade do Porto, rua Dr. Roberto Frias, 4200-465 Porto, Portugal.

Corresponding author email address: mendes@fe.up.pt

Fig. S1 - **S15**.

Table S1 - **S4**

(**a**)

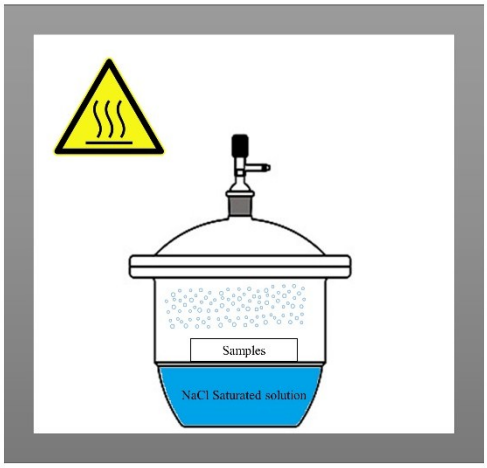

(**b**)

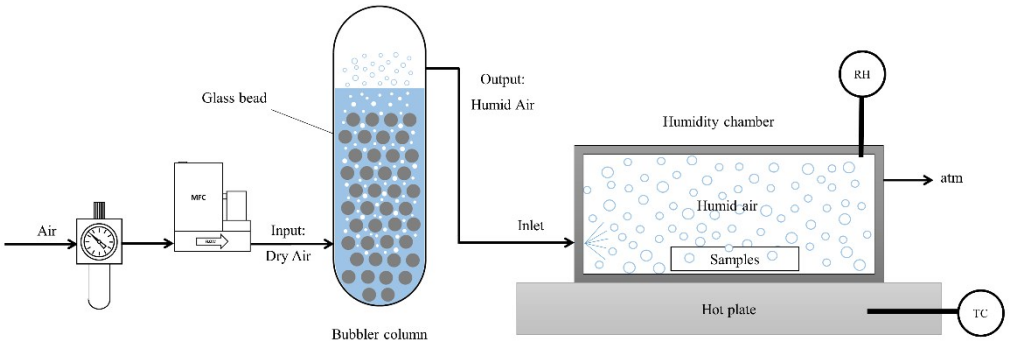

Fig. S1. Schematic view of (**a**) saturated salt solution environment and (**b**) humid air feeding chamber apparatus.

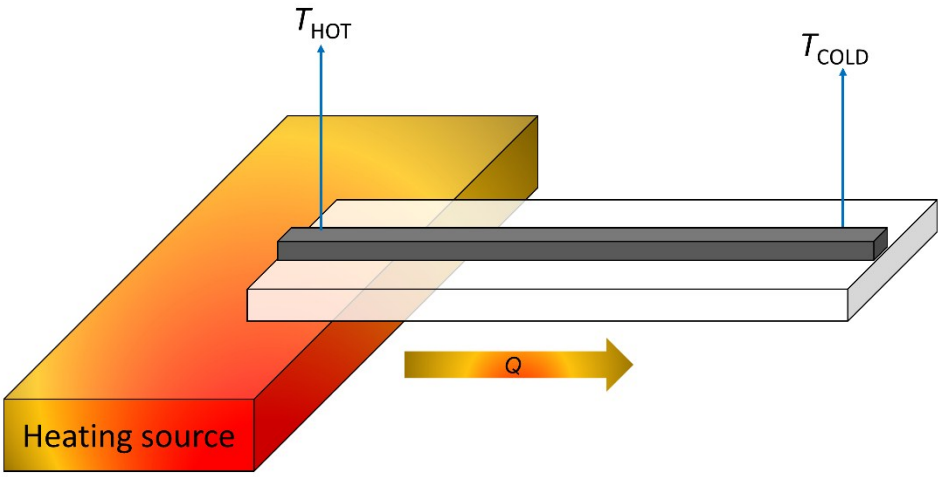

Fig. S2. Schematic view of in-house apparatus for thermal conductivity comparison measurements. Samples with similar glass substrate and glass frit dimensions were used to compare the thermal conductivity of glass frits.

Fourier's law of heat conduction:

$$Q = -kA\frac{\Delta T}{\Delta x}$$

where; Q is the heat transfer rate, $\frac{\Delta T}{\Delta x}$ is the temperature gradient in the direction of the heat flow, A is area, and k is the thermal conductivity.

$$k = -\frac{Q\,\Delta x}{A}\frac{1}{\Delta T}$$

for equal heat transfer rate and sample size, the thermal conductivity is proportional to the reciprocal of the ΔT:

$$K \propto \frac{1}{\Delta T}$$

(**a**)

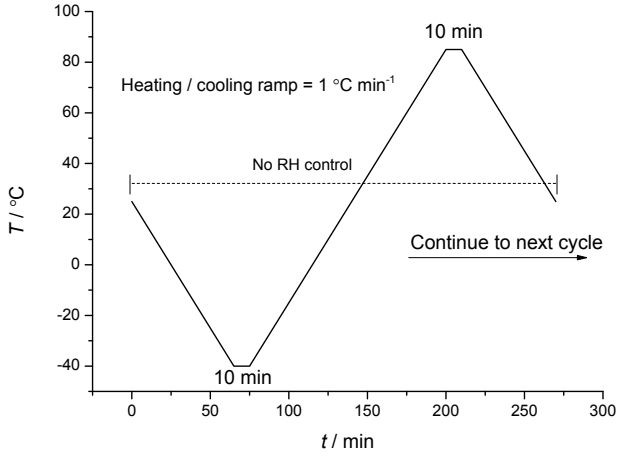

(**b**)

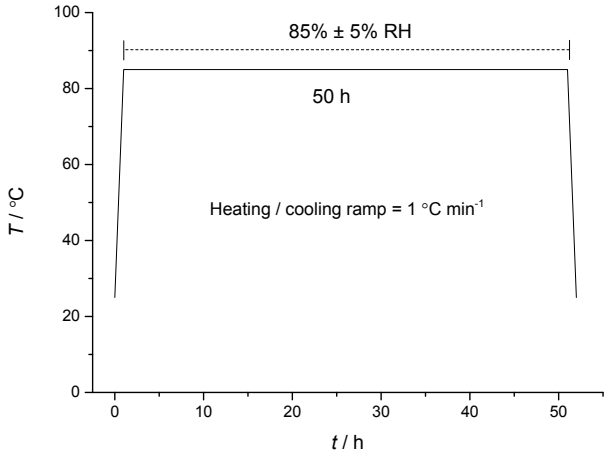

Fig. S3. Temperature and humidity history for (**a**) thermal cycle and (**b**) damp heat test according to IEC61646.

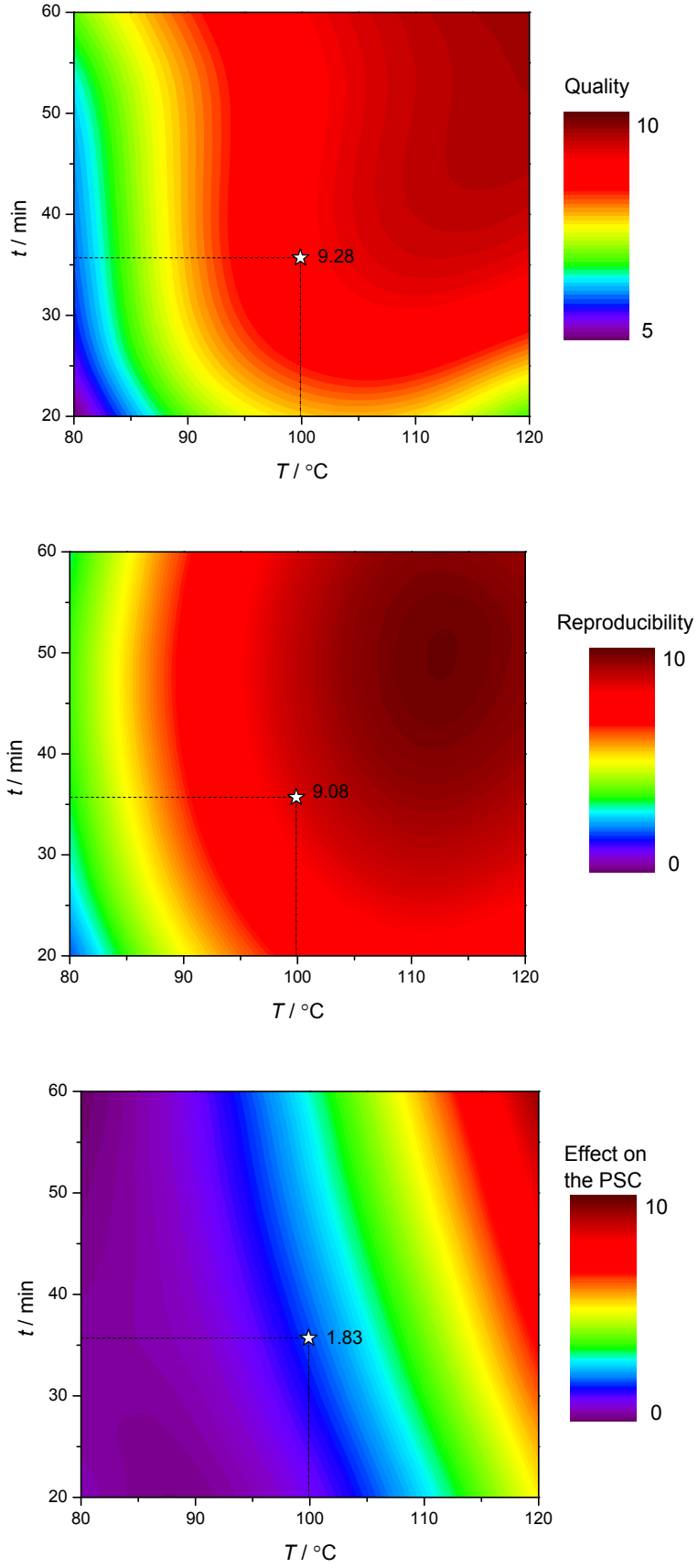

Fig. S4. Contour plots for predicted response functions of the RSM model.

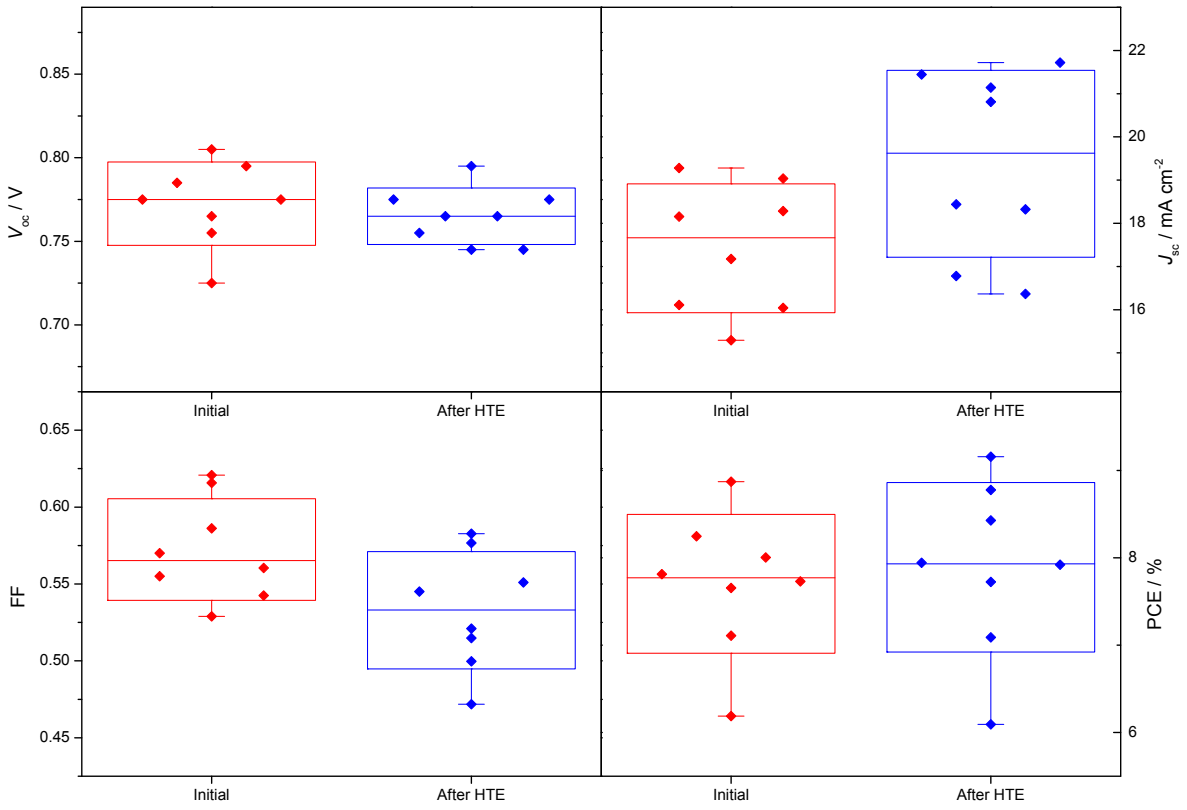

Fig. S5. 50 h of 70 % RH Humidity and temperature (40 °C) exposure (HTE) effect on the photovoltaic parameters of the devices.

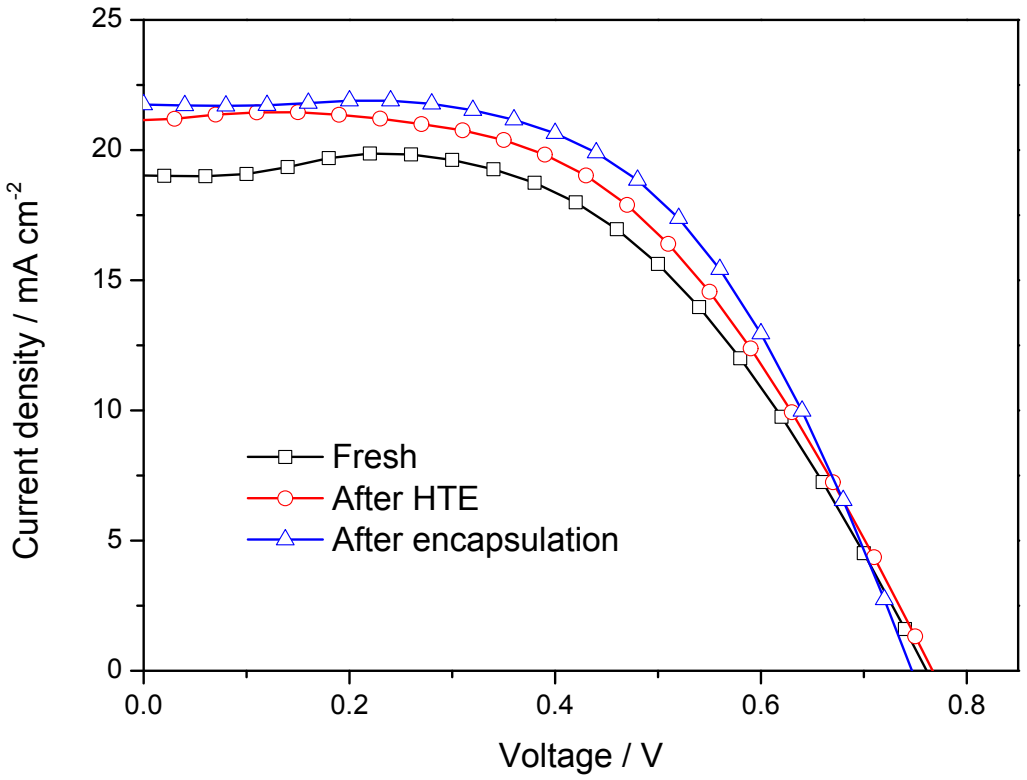

Fig. S6. *J-V* curve for an average performance cell (4 mV s^{-1}, reverse bias); fresh, after HTE and after encapsulation.

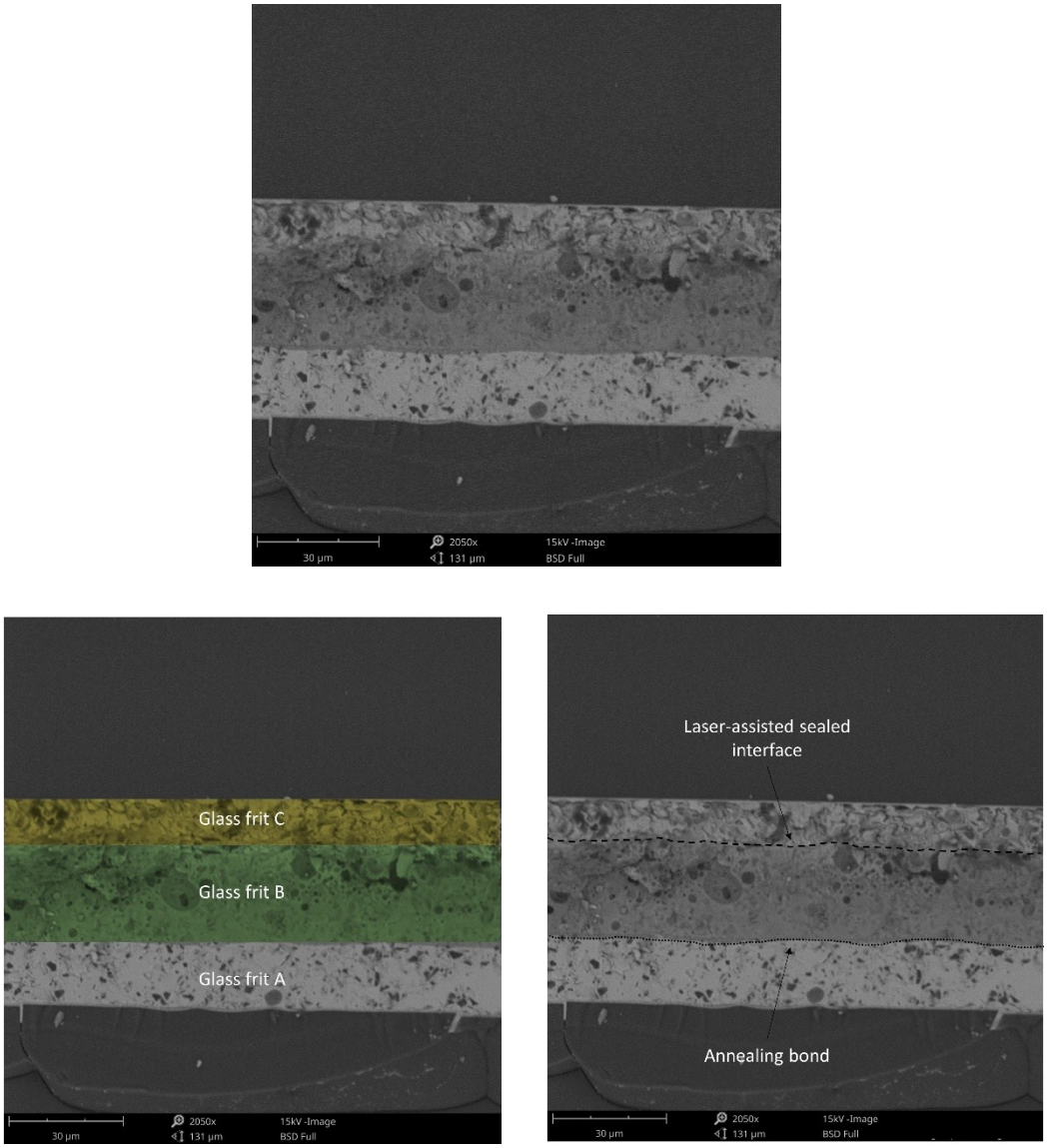

Fig. S7. SEM image of the triple layer glass frit encapsulation for PSC device.

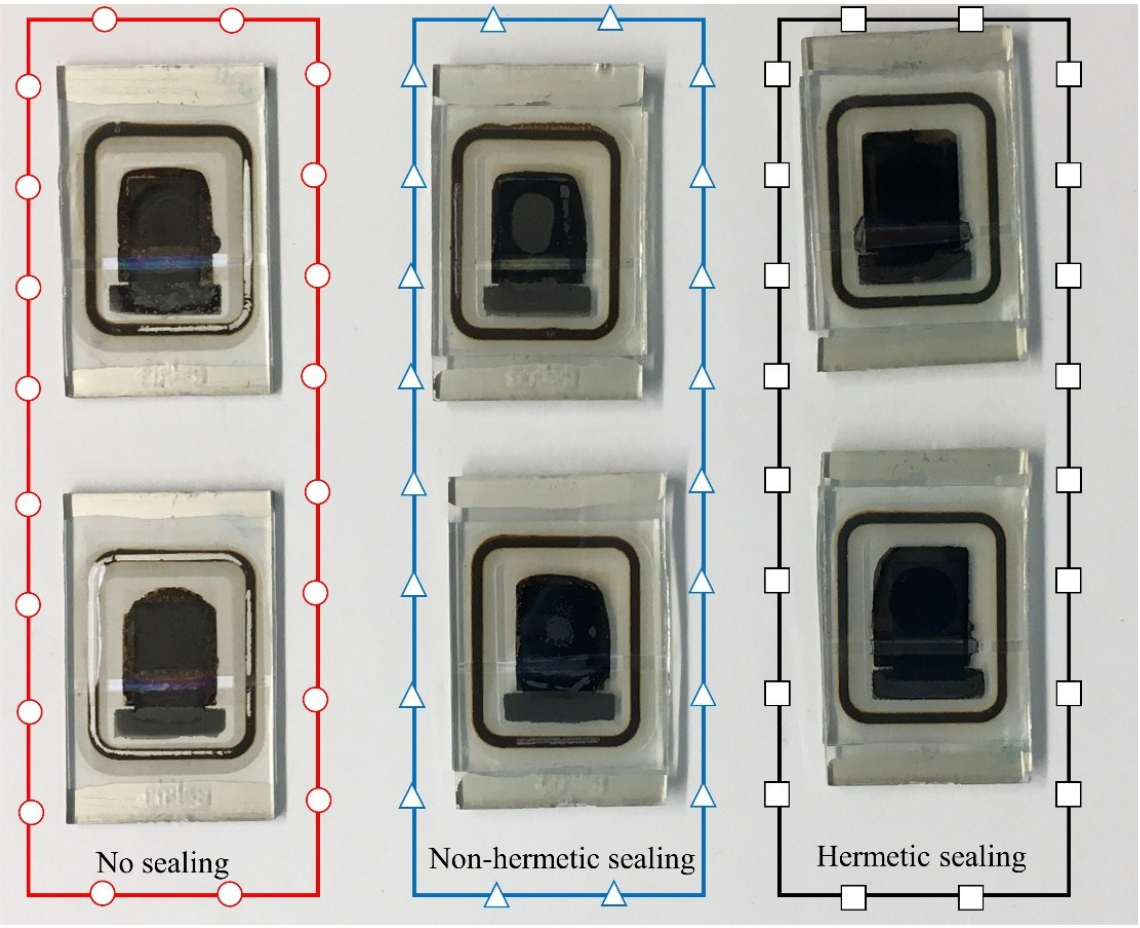

Fig. S8. Photograph of devices after the humidity aging test; no sealing (40 h), non-hermetic sealing (135 h) and hermetic sealing (500 h).

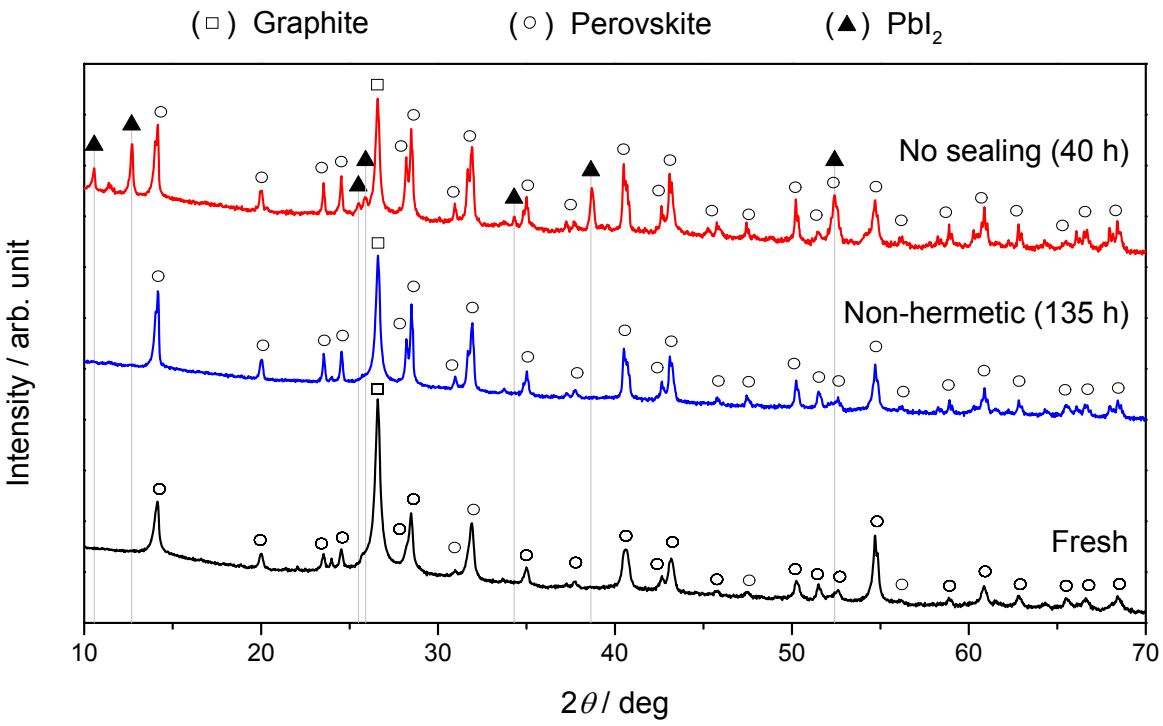

Fig. S9. XRD patterns of complete device (glass/FTO/TiO_2/ZrO_2/$(5\text{-AVA})_{0.05}(MA)_{0.95}PbI_3$); fresh, “no sealing” and “non-hermetic” after 40 h and 135 h of humid air feeding test.

(**a**)

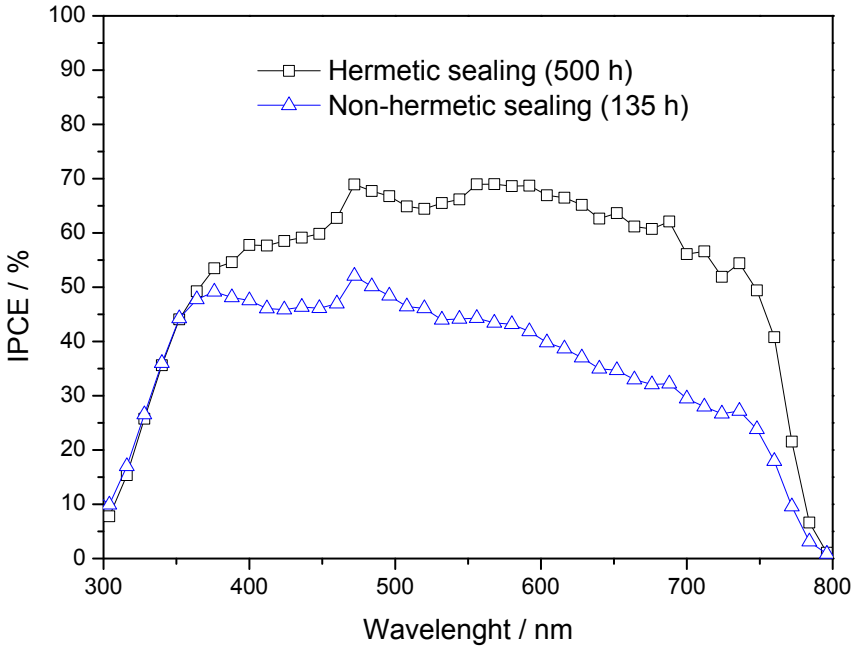

(**b**)

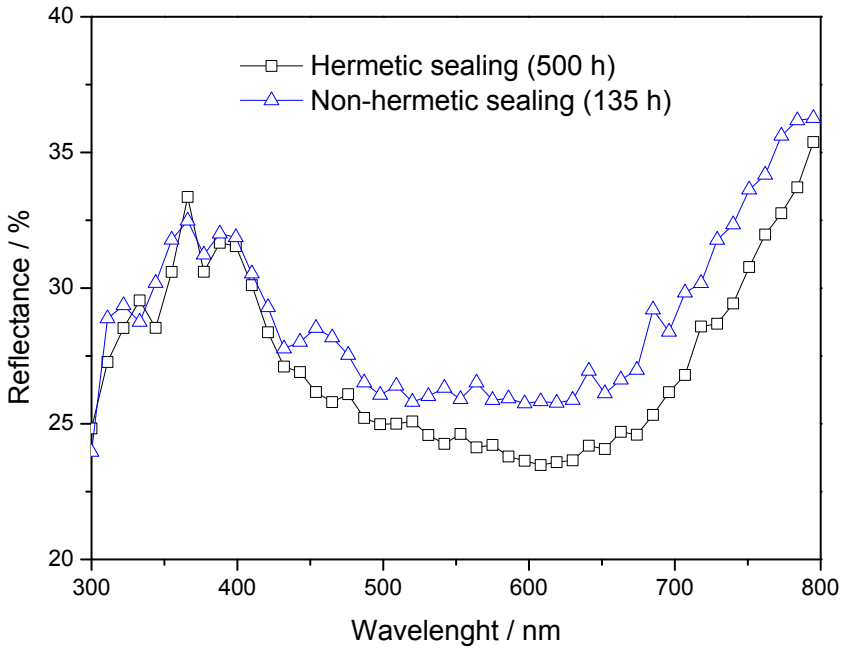

Fig. S10. (**a**) IPCE (without biased light) and (**b**) reflectance for aged hermetic and non-hermetic sealing devices.

(**a**)

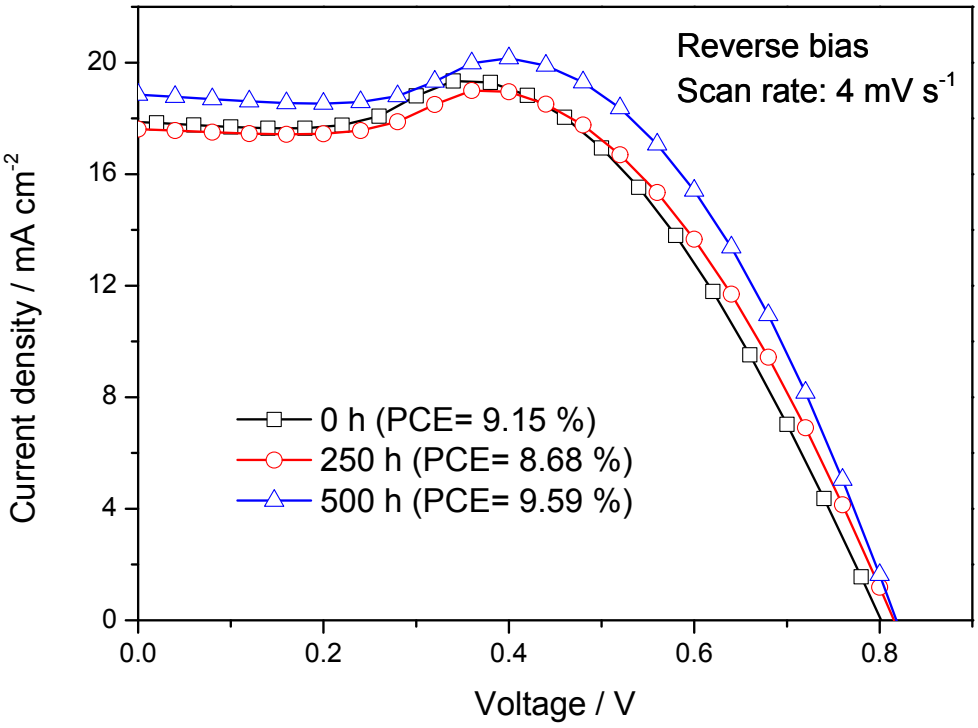

(**b**)

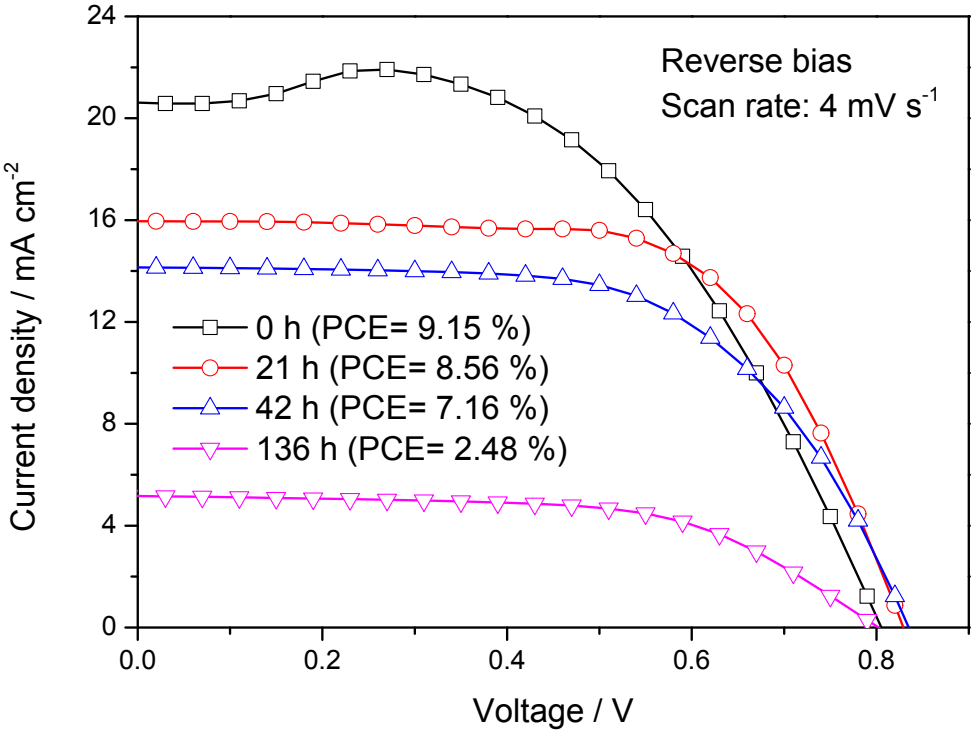

Fig. S11. *J-V* curves for (**a**) hermetic and (**b**) non-hermetic sealed PSCs during humid air feeding stability test.

(**a**)

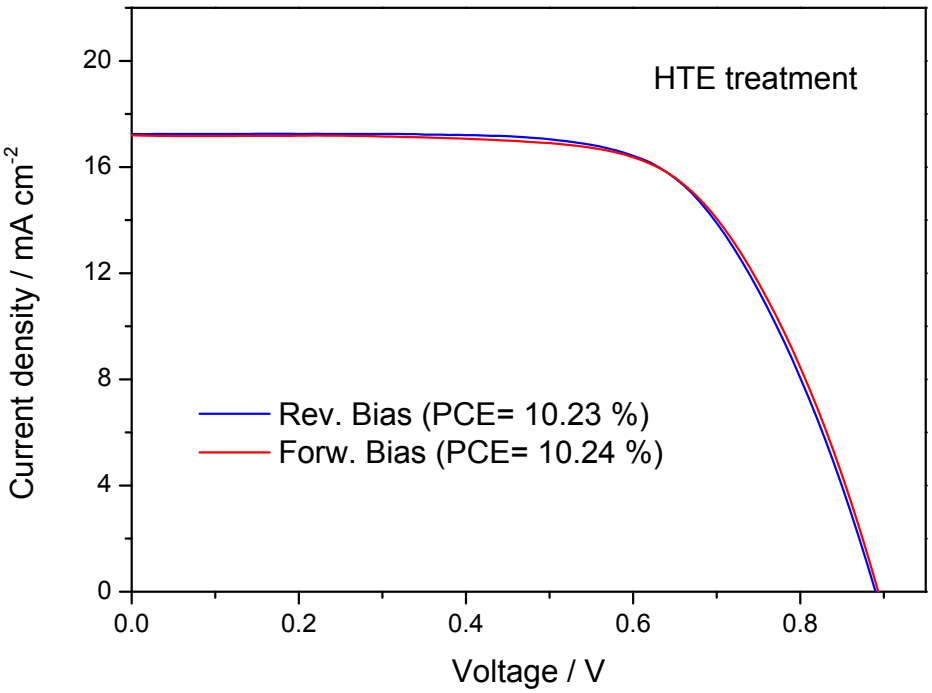

(**b**)

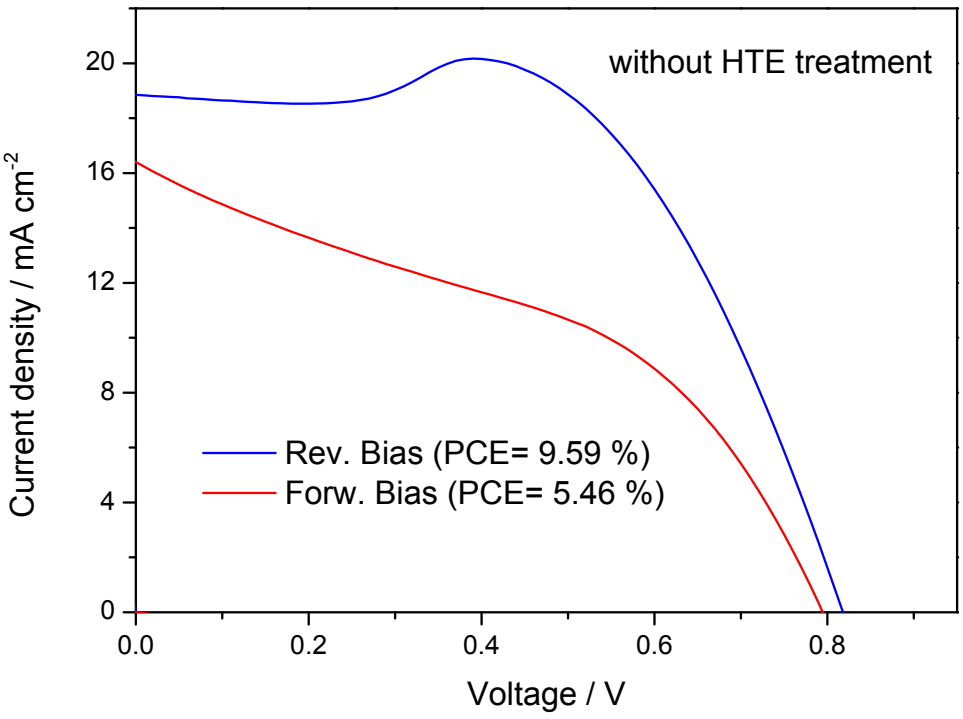

Fig. S12. *J-V* curves (scan rate: 4 mV s^{-1}) for encapsulated device (**a**) with HTE (**b**) without HTE.

(**a**)

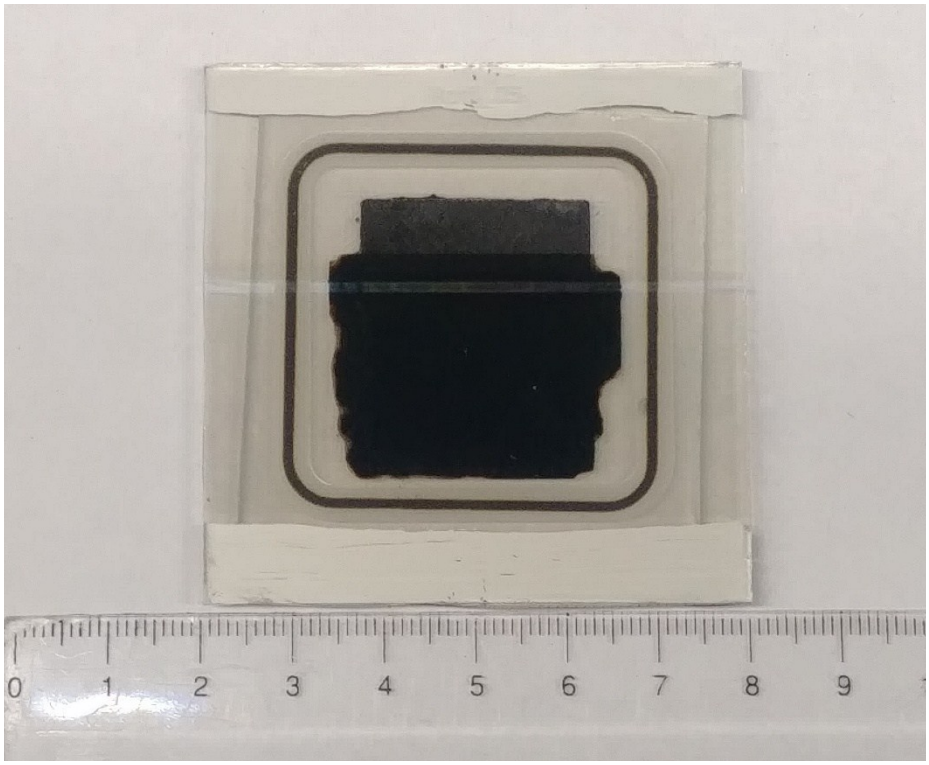

(**b**)

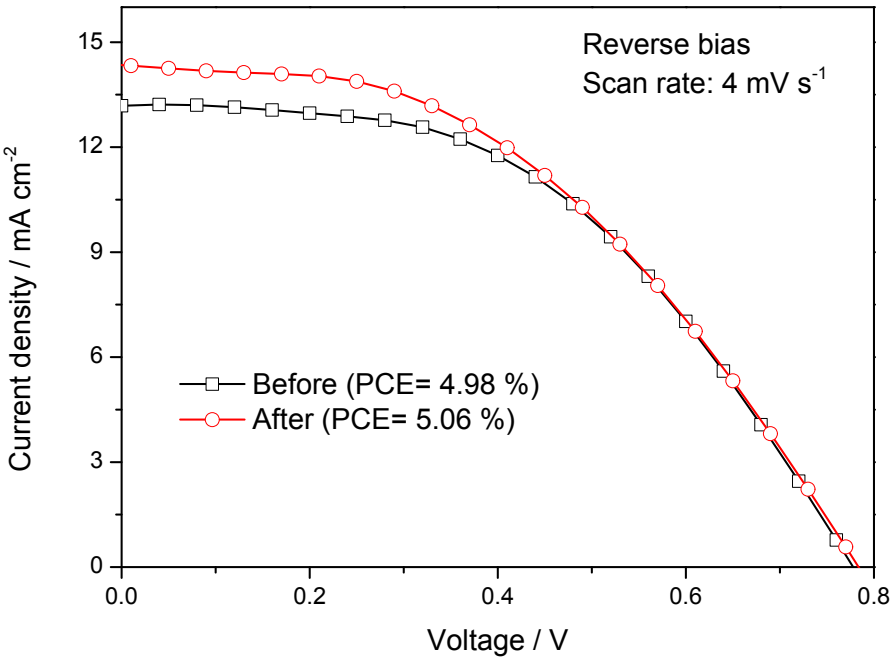

Fig. S13. (**a**) Photograph and (**b**) *J-V* curve (scan rate: 4 mV s^{-1}) for a large area encapsulated device (before and after encapsulation).

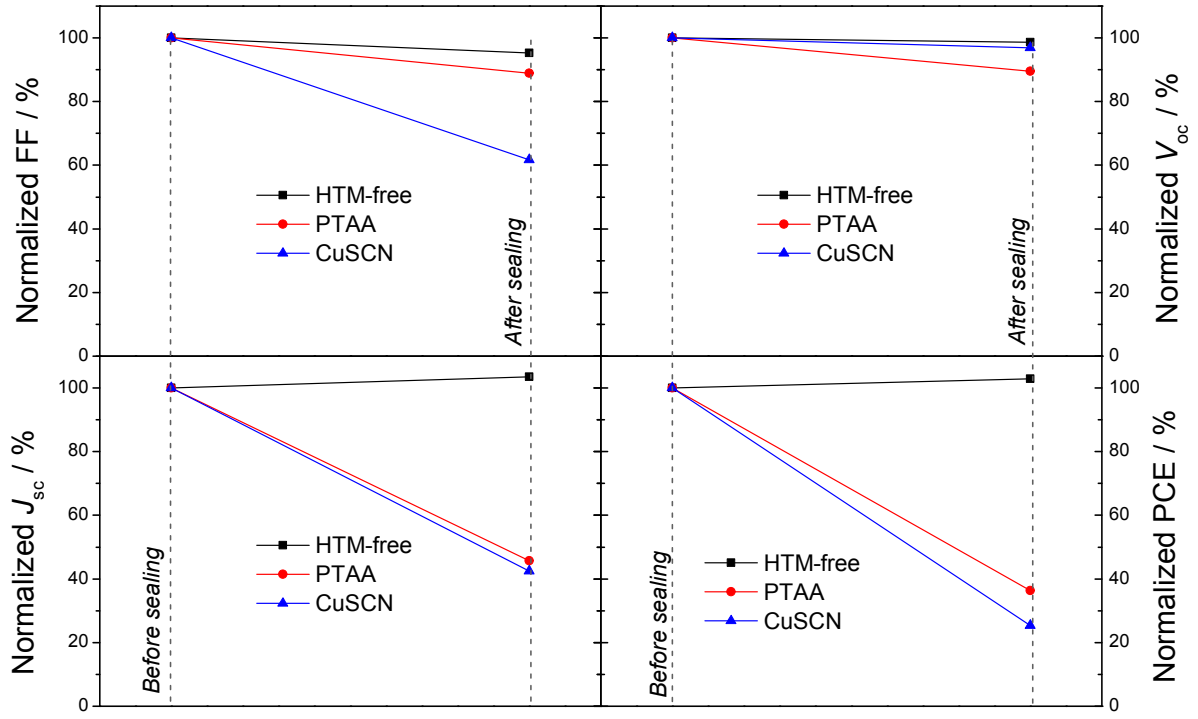

Fig S14. Effect of encapsulation process (100 °C, 35 min) on photovoltaic parameters of HTM-free *vs*. HTM-based PSCs.

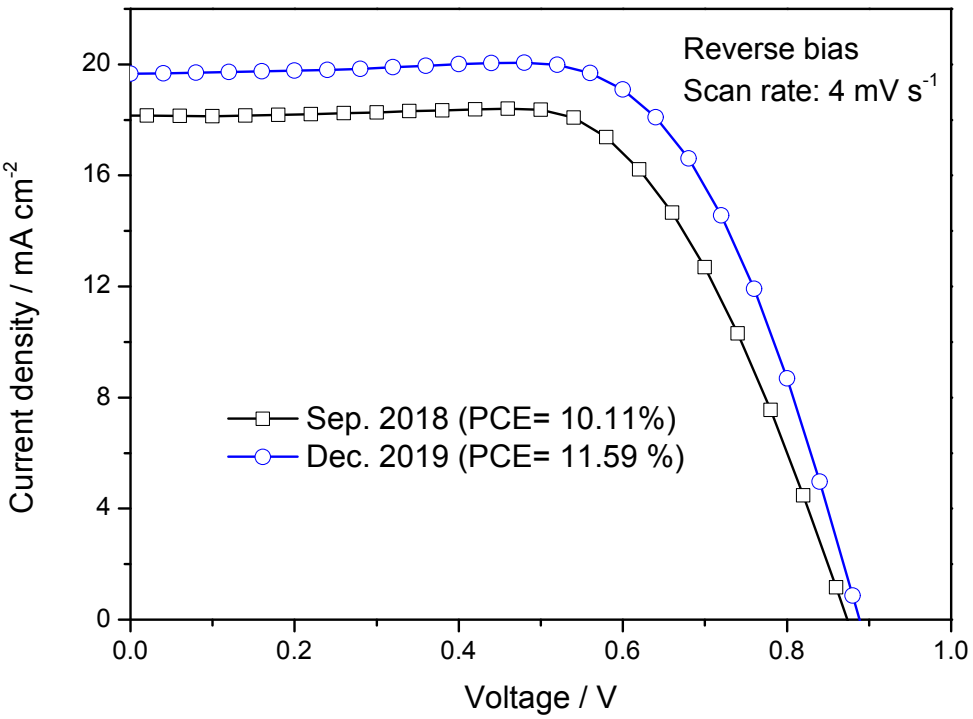

Fig S15. *J-V* curves for an encapsulated HTM-free device after 15 months of fabrication. The device was stored in dark at normal atmospheric condition. As mentioned, the performance of HTM-free PSCs improves during several days after the fabrication date.

Table S1. Chemical composition and properties of the glass frits.

Glass frit	Composition	CTE × 10^{-6} / K^{-1}	Thermal conductivity / arb. Unit	Bonding temperature / °C
A	$SiO_2 \cdot B_2O_3 \cdot PbO$	7.8	++	430
B	$TeO_2 \cdot V_2O_5$	8.0	+++	380
C	$BaO \cdot SiO_2 \cdot PbO \cdot Ag$	9.0	++++	450
D	$BaO \cdot SiO_2 \cdot PbO$	7.9	++	450
E	$Bi_2O_3 \cdot ZnO$	7.7	+	440
F	$SiO_2 \cdot Bi_2O_3 \cdot ZnO$	7.5	+	450

Table S2. Laser-assisted sealing condition for various encapsulation configurations.

Glass frit configuration	Overall thermal shock resistance	$T_{bonding}$ /°C	$T_{process}$ / °C	$\Delta T_{LA,minimum}$ / °C	Remarks	Ref.
A-A	++	430	250	180	High $T_{process}$; not suitable for PSCs.	Present work
B-B	+++	380	120	260	Low sealing reproducibility.	Present work
C-C	+++++	450	25	425	Electrically conductive; not suitable for PSCs.	[1]
C-C	+++++	450	120	330	Electrically conductive; not suitable for PSCs.	[1]
D-D	++	450	250	200	High $T_{process}$; not suitable for PSCs.	Present work
E-E	+	440	330	110	High $T_{process}$; not suitable for PSCs.	Present work

F-F	+	450	330	120	High $T_{process}$; not suitable for PSCs.	[2]
C-B	+++	380	120	260	Suitable for PSCs; major negative effect on device performance.	[3]
C-BA	++++	380	100	280	Suitable for PSCs; minimal negative effect on device performance.	Present work

Table S3. Factors, intervals and goals for response surface methodology (RSM) method for sealing process optimization.

Factor (variable/ response)		**Interval**		**Optimization goal**
		Lower limit	Upper limit	
Sealing process temperature / °C	Variable	80	120	In range
Sealing dwell time / min	Variable	20	60	In range
Sealing quality	Response	0	10	Maximize (weight = 0.375)
Reproducibility	Response	0	10	Maximize (weight = 0.125)
Effect on the PSC	Response	0	10	Minimize (weight = 0.5)

Table S4. Response function, R-squared adjusted, and R-squared of the RSM model. The *p*-value of all three responses are < 0.0001.

Predicted response function	R_{Adj}^2	R^2
Quality = -76.02 + 1.82 T + 0.57 t - 7.53 × 10 $^{-3}$ tT - 0.01 T^2 - 4.26 × 10^{-3} t^2 + 7.19 × 10^{-5} T^2t - 7.67 × 10^{-5} Tt^2 + 2.13 × 10^{-5} T^3 + 8.67 × 10^{-5} t^3	0.97	0.78
Reproducibility = -71.92 + 1.36 T + 0.02 t + 4.66 × 10^{-4} tT - 6.16 × 10^{-3} T^2 - 2.57 × 10^{-3} t^2	0.95	0.87
Effect on device = 42.2 - 0.91 T - 0.24 t + 3.10 × 10^{-3} tT + 4.88 × 10^{-3} T^2 - 1.43 × 10^{-4} t^2	0.94	0.88

References

[1] S. Emami, J. Martins, L. Andrade, J. Mendes and A. Mendes, *Optics and Lasers in Engineering*, 2017, **96**, 107-116.

[2] F. Ribeiro, J. Maçaira, R. Cruz, J. Gabriel, L. Andrade and A. Mendes, *Solar Energy Materials and Solar Cells*, 2012, **96**, 43-49.

[3] S. Emami, J. Martins, R. Madureira, D. Hernandez, G. Bernardo, J. Mendes and A. Mendes, *Journal of Physics D: Applied Physics*, 2019, **52**, 074005.